

## NOTE

### The Abundance of AsH<sub>3</sub> in Jupiter

KEITH S. NOLL AND HAROLD P. LARSON

*Lunar and Planetary Laboratory, University of Arizona, Tucson, Arizona 85721*

AND

T. R. GEBALLE

*Joint Astronomy Centre, 665 Komohana Street, Hilo, Hawaii 96720*

Received August 28, 1989; revised November 2, 1989

**We derive a new estimate of the arsenic abundance in Jupiter from ground-based and airborne observations in the region of the AsH<sub>3</sub> Q-branch at 2126 cm<sup>-1</sup>. We used newly analyzed laboratory comparison spectra at AsH<sub>3</sub> to determine that the mole fraction of AsH<sub>3</sub> in Jupiter's atmosphere is  $0.22 \pm 0.11$  ppb, only 0.5 times the solar abundance and nine times less than the mole fraction found in Saturn. The relative abundance of arsenic in these two planetary atmospheres follows the same pattern found for phosphorous. This similarity may constrain models for the incorporation of heavy elements into the gaseous envelopes of the outer planets.** © 1990 Academic Press, Inc.

#### INTRODUCTION

Arsine gas (AsH<sub>3</sub>) was recently detected in Saturn and Jupiter (Noll *et al.* 1989, Bézard *et al.* 1989). The amount of AsH<sub>3</sub> found in Saturn by each group ( $\approx 2$  ppb) agrees within the errors (factor of  $\approx 2$  uncertainty), but the two groups disagree on the AsH<sub>3</sub> abundance in Jupiter. Noll *et al.* estimated that the jovian AsH<sub>3</sub> abundance was  $0.7^{+0.7}_{-0.4}$  ppb from a composite of several spectra obtained at the United Kingdom Infrared Telescope (UKIRT) by comparing the optical depth of the planetary feature to low-pressure laboratory spectra of AsH<sub>3</sub> (Larson 1988, private communication). Bézard *et al.* reanalyzed published high-altitude spectra of Jupiter (cf. Bjoraker *et al.* 1986) using model calculations with AsH<sub>3</sub> molecular line parameters (Tarrago *et al.* 1987) and found evidence for an AsH<sub>3</sub> mole fraction of  $q_{\text{AsH}_3} \leq 0.3$  ppb. (Treffers *et al.* (1978) previously searched this same spec-

trum for AsH<sub>3</sub>, but without the aid of models, and set an upper limit of  $q_{\text{AsH}_3} < 5$  ppb.) We report in this Note a revised estimate of the abundance of AsH<sub>3</sub> in Jupiter based on airborne and new ground-based spectra analyzed with atmospheric models containing AsH<sub>3</sub>.

#### OBSERVATIONS

In order to improve the determination of Jupiter's AsH<sub>3</sub> abundance, we obtained two new spectra of Jupiter from UKIRT on 1989 January 28 using the UKIRT Fabry–Perot spectrometer (FP) in the spectral interval 2119.7–2132.6 cm<sup>-1</sup> at 0.22 cm<sup>-1</sup> resolution. A 5" diameter aperture was centered on Jupiter's North Equatorial Belt (NEB) for one series of scans and on the cloudier Equatorial Zone (EqZ) for another. The star BS 1017 (0.437 mag at 4.63  $\mu\text{m}$ , Gezari *et al.* 1987) was used to eliminate telluric absorptions and to provide absolute flux calibration, which we estimate

to be accurate within 20%. The final ratioed spectra of the NEB and EqZ have signal-to-noise ratios (S/N) of 35 and 17, respectively. We removed a small slope ( $\approx 12\%$ ) in the continuum of the NEB scan that became apparent when compared to the EqZ spectrum, previous UKIRT data (Noll *et al.* 1989), and the airborne observations described below. Anomalous slopes of this magnitude sometimes result from slowly varying atmospheric transmission, flexure in the telescope, and other difficulties in tracking the NEB hot spots.

Although the new UKIRT spectra have broader spectral coverage ( $\approx 13 \text{ cm}^{-1}$ ) than the composite spectrum presented in Noll *et al.* (1989) ( $\approx 8 \text{ cm}^{-1}$ ), significant uncertainties apply to model simulations of such narrow spectral intervals because of the competing influences of cloud and molecular opacities. To minimize this uncertainty we included in our analysis the broadband spectrum of Jupiter obtained with a Fourier transform spectrometer (FTS) on the Kuiper Airborne Observatory (KAO) during 1975 December. The spectrum covers the entire Jovian atmospheric transmission window ( $1800\text{--}2250 \text{ cm}^{-1}$ ) at  $5 \text{ }\mu\text{m}$  at a spectral resolution of  $0.5 \text{ cm}^{-1}$  (unapodized) and has a peak S/N  $\approx 100$ . These data first appeared in Larson *et al.* (1977) and were more recently interpreted by Bjoraker *et al.* (1986) and Bézard *et al.* (1989). We divided the Jovian spectrum by a lunar comparison spectrum normalized to a blackbody temperature of 240 K (Bjoraker 1985) to remove instrumental transmission characteristics and residual telluric absorptions. We normalized the KAO data to the UKIRT NEB observations at  $2130.4 \text{ cm}^{-1}$  in order to compare the two planetary spectra directly. Normalization in this way is valid because the whole disk spectrum is dominated by emission from warm regions such as the NEB and because it has been shown that the cloud attenuating Jupiter's  $5\text{-}\mu\text{m}$  radiation adds negligible radiation of its own to the outgoing flux even in cold zones (Noll *et al.* 1988).

## ANALYSIS

The UKIRT NEB spectrum and a section from the KAO spectrum are shown in Fig. 1 along with three synthetic spectra calculated with 0.0, 0.3, and 0.7 ppb of  $\text{AsH}_3$  respectively. The radiative transfer program and molecular line parameters are described in Noll (1987). In addition, we included the molecular line list for  $\text{AsH}_3$  generated by G. Tarrago and co-workers (Bézard 1988, private communication). The observed spectra are displaced from each other in Fig. 1 so that they may be separately compared to model calculations. Although the observations differ by a factor of  $\approx 2$  in spectral resolution, the planetary features are very similar in each spectrum due to the combined effects of pressure-broadened line widths and the superposition of many planetary absorption lines. The synthetic spectra were computed on a  $0.05\text{-cm}^{-1}$  grid and then convolved with instrumental functions appropriate to each spectrometer (a Lorentz function for the FP and a sinc function for the FTS). The molecular abundances were those used by Bjoraker *et al.* (1986), except for CO (1.3 ppb) and  $\text{GeH}_4$  (0.5 ppb). A baseline model with 0.3 ppb of  $\text{AsH}_3$  was computed from  $2000\text{--}2250 \text{ cm}^{-1}$  and scaled to minimize the mean square deviation between the observed and calculated spectra. This procedure is insensitive to the assumed  $\text{AsH}_3$  abundance because  $\text{AsH}_3$  absorption is important only over a  $\approx 5\text{-cm}^{-1}$ -wide-interval.

The three model calculations in Fig. 1 illustrate spectra with no  $\text{AsH}_3$ , the baseline amount of 0.3 ppb, and that estimated by Noll *et al.* (0.7 ppb). We also calculated models with 0.1, 0.2, and 0.4 ppb of  $\text{AsH}_3$  that are not shown in Fig. 1. The synthetic spectra exhibit large changes in the region near  $2126 \text{ cm}^{-1}$ , the location of the  $\nu_3$  Q-branch of  $\text{AsH}_3$  and modest variation near  $2114 \text{ cm}^{-1}$ , the position of the  $\nu_1$  Q-branch, for  $\text{AsH}_3$  abundances in the range 0.0–0.7 ppb. We base our analysis only on the  $2126\text{-cm}^{-1}$  feature since it is common to the

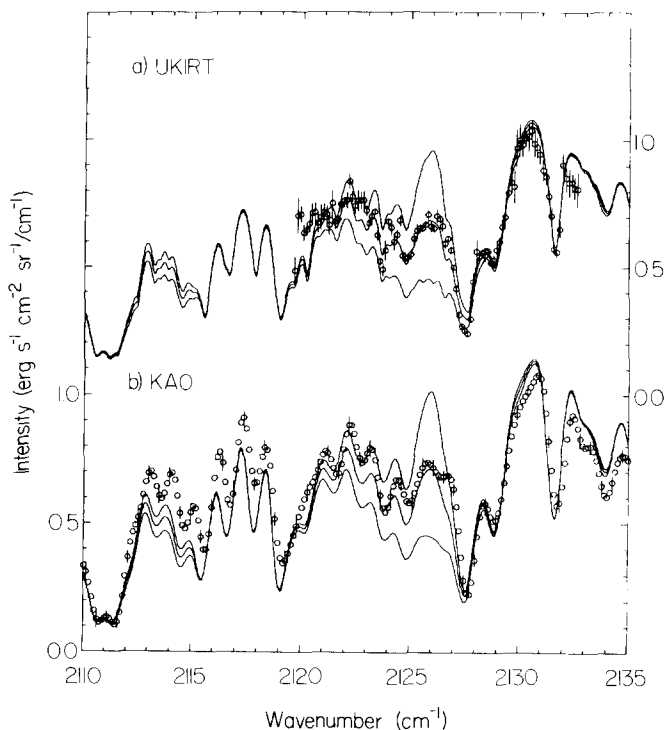


FIG. 1. (a) Spectrum of the jovian NEB obtained with the UKIRT Fabry–Perot spectrometer at a resolution of  $0.22\text{ cm}^{-1}$ . (b) Spectrum of the central  $25''$  of the jovian disc obtained from the KAO at a spectral resolution of  $0.5\text{ cm}^{-1}$ . Circles without error bars are points interpolated from the primary data with a sinc function. Three synthetic spectra (solid lines) are compared with each observation to demonstrate the effects of varying abundances of  $\text{AsH}_3$ : the upper solid curve has no  $\text{AsH}_3$ , the middle has a mole fraction of  $0.3\text{ ppb}$ , and the lower curve has  $0.7\text{ ppb}$ . The greatest sensitivity to the detection of  $\text{AsH}_3$  occurs near  $2126\text{ cm}^{-1}$ , the position of the  $\nu_3$  Q-branch. The weaker  $\nu_1$  Q-branch at  $2114\text{ cm}^{-1}$  has a smaller effect on the spectrum.

UKIRT and KAO data. The diagnostic value of the weaker  $\nu_1$  band is limited by the model's inability to match the continuum level in all regions of the KAO spectrum (see discussion below) and because the  $\nu_1$  Q-branch does not produce a distinctive spectral signature but rather a level change not much larger than the error bars. The best fit  $\text{AsH}_3$  abundance is closer to that in the baseline spectrum than in the two extreme cases included in Fig. 1. The calculated residuals indicate a best fit value of  $0.26\text{ ppb}$  for the UKIRT NEB data and  $0.17\text{ ppb}$  for the KAO spectrum. A similar value (but with significantly greater uncertainty) is obtained for the EqZ data, as expected, since

this spectrum matches the NEB spectrum to within the noise levels when they are normalized at  $2130.4\text{ cm}^{-1}$ . The individual spectra are fit to  $\pm 0.05\text{ ppb}$ , however, the variations among the values derived from separate data sets,  $\pm 0.09\text{ ppb}$ , may be a fairer estimate of the uncertainty in the data as well as the modeling and fitting procedure. In addition, the  $\text{AsH}_3$  line strengths carry a 30% uncertainty (Bézard *et al.* 1989). Combining these errors and giving equal weight to the UKIRT and KAO spectra we conclude that the mole fraction of  $\text{AsH}_3$  in Jupiter is  $q_{\text{AsH}_3} = 0.22 \pm 0.11\text{ ppb}$ .

Numerous small, but potentially significant, differences exist between the airborne

spectrum and the baseline model, such as in the spectral interval near  $2114\text{ cm}^{-1}$  and others that are not shown in Fig. 1. In view of these differences, Bézard *et al.* (1989) urged some caution in accepting the identification of AsH<sub>3</sub> in Jupiter. However, several arguments support the assignment of AsH<sub>3</sub> to the absorption feature at  $2126\text{ cm}^{-1}$  in Jupiter's spectrum. First, this feature is similar to one observed in Saturn where additional AsH<sub>3</sub> lines have been detected, leaving no doubt about its identification there (Bézard *et al.* 1989, Noll and Larson, in preparation). Second, the addition of AsH<sub>3</sub> to the atmospheric model reproduces not just the overall flux level, but matches the spectral shape in detail, a feat that would be difficult to reproduce in any other way. Third, the spectral feature that we associate with the  $\nu_3$  Q-branch of AsH<sub>3</sub> occurs reproducibly in multiple independent observations of Jupiter (three UKIRT scans and one KAO spectrum). Taken together, these points constitute compelling evidence for AsH<sub>3</sub> in Jupiter at the 0.2 ppb level. Finally, the derived AsH<sub>3</sub> abundance is plausible from cosmochemical (Cameron 1982) and planetary thermodynamic (Barshay and Lewis 1978) theoretical arguments.

The importance of the differences elsewhere in Jupiter's  $5\text{-}\mu\text{m}$  spectrum to jovian atmospheric chemistry should not be ignored, however. We speculate that some discrepancies between models and observations might be reduced by adjusting the abundances of other atmospheric gases, while others may be signatures of still unidentified absorbers or the result of uncertainties in the molecular line parameters of known absorbers, particularly PH<sub>3</sub>. Treating clouds as gray absorbers rather than multiple scattering media also leads to errors (Carlson *et al.* 1988). Scattering is likely to produce subtle slope changes between strong line and weak line regions of the spectrum, but in general these effects vary slowly with frequency. The investigation of all of these possibilities goes beyond the scope of this paper, but we note that

refinements to existing  $5\text{-}\mu\text{m}$  atmospheric models are not likely to affect the derived abundance of AsH<sub>3</sub> substantially. However, it may be possible to estimate the magnitude of uncertainty introduced by the current limitations in producing model spectra at  $5\text{ }\mu\text{m}$  and other wavelengths by comparing  $5\text{ }\mu\text{m}$  abundances to molecular abundance determinations in other spectral regions where details of the radiative transfer are much different. For example, in spectra at  $1100\text{--}1200\text{ cm}^{-1}$  Knacke *et al.* (1982) found an NH<sub>3</sub> abundance equal to the value derived from  $5\text{-}\mu\text{m}$  data, and PH<sub>3</sub> and CH<sub>3</sub>D abundances 20 and 80% greater than  $5\text{-}\mu\text{m}$  determinations, respectively. This and similar examples indicate that the approximations made in  $5\text{-}\mu\text{m}$  models are adequate given the current uncertainties in observations and laboratory data, although future improvements may require better modeling of multiple scattering and clouds.

An additional result of the model calculations is some information on the jovian cloud layers. The model contains a cloud at 190 K with variable gray opacity. Changes in this opacity result in simple scaling of the output as virtually all of the radiation originates in deeper and hotter portions of the atmosphere ( $P \approx 7$  bars,  $T \approx 300$  K, Noll *et al.* 1988). This model cloud simulates the combined effects of the putative NH<sub>3</sub> and NH<sub>4</sub>SH cloud decks. We found that the total cloud opacity was  $\tau = 1.27$  for the NEB model and  $\tau = 2.39$  for the EqZ. These values are typical of cloud opacities derived from other observations at  $5\text{ }\mu\text{m}$  (Drossart *et al.* 1982, Bjoraker 1985, Noll *et al.* 1988), although the physical significance of these optical depths is not yet clear.

#### DISCUSSION

Fegley (1988) recently confirmed the prediction by Barshay and Lewis (1978) that small amounts of vertical mixing in planetary atmospheres are sufficient to prevent depletion of AsH<sub>3</sub> in their upper tropospheres by chemical reactions. As mentioned above, the radiation we observe

comes from the  $P \approx 7$  bar level, making the column abundance insensitive to assumed details of photodissociation at  $P < 500$  mbar. The observed amount of  $\text{AsH}_3$  therefore represents the global abundance of arsenic in Jupiter's gaseous envelope. The arsenic abundance in Jupiter compared to solar and meteoritic abundances may be expressed by the enrichment factor  $\rho = (\text{As}/\text{H})_J/(\text{As}/\text{H})_\odot$ . We find that  $\rho = 0.53 \pm 0.34$  using  $(\text{As}/\text{H})_\odot = 0.23$  ppb (Cameron 1982).

Our derived abundance of  $\text{AsH}_3$  in Jupiter is remarkable on two counts. First, it is the lowest concentration of a trace atmospheric constituent yet detected in the outer planets and testifies to the continuing progress in laboratory, computational, and observational studies of the solar system. Second,  $\text{AsH}_3$  is nine times less plentiful in Jupiter than in Saturn. This result leaves no doubt that Saturn is greatly enriched in heavy elements relative to Jupiter. As noted by Noll *et al.* (1989), the relative enrichments of arsenic and phosphorous are similar in Jupiter and Saturn. Both apparently differ from the enrichment pattern of carbon (Gautier and Owen 1989), a fact that may be of significance in models of planetary formation. Our new  $\text{AsH}_3$  determination for Jupiter strengthens these conclusions.

In core-instability models of the formation of the outer planets (e.g., Stevenson 1982), heavy element abundances in the gaseous envelope need not bear any similarity to a solar mixture of elements, as our use of the term enrichment may erroneously suggest. The abundance of an element in the gaseous envelope depends, instead, on presently unknown details of the formation process. The ratio of envelope mass to core mass is lower in Saturn than in Jupiter (Hubbard and Marley 1989). If heavy elements in the envelope come originally from core material, one would then expect greater heavy-element abundances in Saturn compared to Jupiter, as observed. One plausible mechanism for infusing heavy elements into the hydrogen-helium

envelop is the dissolution of late-arriving planetesimals in the forming gaseous envelop (Pollack *et al.* 1986). The solid material dissolved in this way is later distributed throughout the atmosphere by convection initiated by the final hydrodynamic collapse of the gaseous nebula component. The measured abundances of arsenic and phosphorous should provide tighter constraints to Pollack *et al.*'s model by eliminating a variable,  $\alpha_i$ , the fraction of element  $i$  that is condensed into solids. Unlike carbon, which Pollack *et al.* considered, and for which  $\alpha$  is unknown, all of the arsenic and phosphorous will be condensed as solids, or  $\alpha = 1$  in Pollack *et al.*'s terminology. Uncertainties about the physical state of ices in the preplanetary nebula (i.e., C, N, and O) are significant, so progress in understanding the early history of the giant planets may depend on continued improvements in cataloging the abundances of the rocky component of the preplanetary nebula.

Finally, we consider the possibility of detecting additional  $\text{AsH}_2$  features in Jupiter's spectrum. No  $\text{AsH}_3$  features besides the  $\nu_3$   $Q$ -branch are detectable at the resolution of existing 5- $\mu\text{m}$  airborne data, although several lines may be observable in spectra at higher resolution. To be found unambiguously, trace constituent species such as  $\text{AsH}_3$  must change the observed shape of spectral features, not simply produce a continuum level change as does the  $\nu_1$   $Q$ -branch of  $\text{AsH}_3$  near  $2114\text{ cm}^{-1}$ . Thus, the detectability of a line depends only partially on its strength. Equally important is the degree of overlap with absorption lines due to other atmospheric constituents. We computed synthetic spectra over the interval  $2000\text{--}2200\text{ cm}^{-1}$  with varying amounts of  $\text{AsH}_3$  and identified three candidates for future work: the P6-, P4-, and R1-lines of the  $\nu_3$  band near 2082, 2097, and  $2141\text{ cm}^{-1}$ , respectively. Detection of these lines could lead to a more accurate determination of Jupiter's arsenic abundance, a number that may be valuable in the effort to understand

the formation and early evolution of the giant planets.

#### ACKNOWLEDGMENTS

We gratefully acknowledge B. Bézard, G. Tarrago, and co-workers for sharing the AsH<sub>3</sub> molecular line list with us. We also thank the United Kingdom Infrared Telescope staff for facilitating our observations. This work was supported in part by NASA Grant NAG 2-206.

#### REFERENCES

- BARSHAY, S. S., AND J. S. LEWIS 1978. Chemical structure of the deep atmosphere of Jupiter. *Icarus* **33**, 593–611.
- BÉZARD, B., P. DROSSART, E. LELLOUCH, G. TARRAGO, AND J.-P. MAILLARD 1989. Detection of arsine in Saturn. *Astrophys. J.* **346**, 509–513.
- BJORAKER, G. L. 1985. The gas composition and vertical cloud structure of Jupiter's troposphere derived from five micron spectroscopic observations. Ph.D., thesis, University of Arizona.
- BJORAKER, G. L., H. P. LARSON, AND V. G. KUNDE 1986. The gas composition of Jupiter derived from 5- $\mu$ m airborne spectroscopic observations. *Icarus* **66**, 579–609.
- CAMERON, A. G. W. 1982. In *Essays in Nuclear Astrophysics* (C. A. Barnes, D. D. Clayton, and D. N. Schramm, Eds.), p 23. Cambridge Univ. Press, Cambridge.
- CARLSON, B. E., A. A. LACIS, AND W. B. ROSSOW 1988. Effect of longitudinal variations in relative humidity on the 5- $\mu$ m spectrum of Jupiter. *Bull. Amer. Astron. Soc.* **20**, 869.
- DROSSART, P., T. ENCRENAZ, V. KUNDE, R. HANEL, AND M. COMBES 1982. An estimate of the PH<sub>3</sub>, CH<sub>3</sub>D, and GeH<sub>4</sub> abundances on Jupiter from the Voyager IRIS data at 4.5  $\mu$ m. *Icarus* **49**, 416–426.
- FEGLEY, M. B. 1988. The chemistry of arsine (AsH<sub>3</sub>) in the deep atmospheres of Saturn and Jupiter. *Bull. Amer. Astron. Soc.* **20**, 879.
- GAUTIER D., AND T. OWEN 1989. In *Origin and Evolution of Planetary and Satellite Atmosphere* (S. K. Atreya, J. B. Pollack, and M. S. Matthews, Eds.), pp. 487–512. Univ. of Arizona Press, Tucson.
- GEZARI, D. Y., M. SCHMITZ, AND J. M. MEAD 1987. Catalog of infrared observations. *NASA Reference Publication* **1196**.
- HUBBARD, W. B., AND M. S. MARLEY 1989. Optimized Jupiter, Saturn, and Uranus interior models. *Icarus* **78**, 102–118.
- KNACKE, R. F., S. J. KIM, S. T. RIDGWAY, AND A. T. TOKUNAGA 1982. The abundances of CH<sub>4</sub>, CH<sub>3</sub>D, NH<sub>3</sub>, and PH<sub>3</sub> in the troposphere of Jupiter derived from high resolution 1100–1200 cm<sup>-1</sup> spectra. *Astrophys. J.* **262**, 388–395.
- LARSON, H. P., R. R. TREFFERS, AND U. FINK 1977. Phosphine in Jupiter's atmosphere: The evidence from high altitude observations at 5 microns. *Astrophys. J.* **211**, 972–979.
- NOLL, K. S. 1987. Carbon monoxide and disequilibrium dynamics in Saturn and Jupiter. Ph.D. thesis, State University of New York at Stony Brook.
- NOLL, K. S., T. R. GEBALLE, AND R. F. KNACKE 1989. Arsine in Saturn and Jupiter. *Astrophys. J. Lett.* **338**, L71–L74.
- NOLL, K. S., R. F. KNACKE, T. R. GEBALLE, AND A. T. TOKUNAGA 1988. The origin and vertical distribution of carbon monoxide in Jupiter. *Astrophys. J.* **324**, 1210–1218.
- POLLACK, J. B., M. PODOLAK, P. BODENHEIMER, AND B. CHRISTOFFERSON 1986. Planetesimal dissolution in the envelopes of the forming giant planets. *Icarus* **67**, 409–443.
- STEVENSON, D. J. 1982. Formation of the giant planets. *Planet. Space Sci.* **30**, 755–764.
- TARRAGO, G., G. POUSSIGUE, N. LACOME, A. LEVY, AND G. GUELACHVILI 1987. Communication FB6 presented at the 42<sup>nd</sup> Symposium on Molecular Spectroscopy, Columbus, OH, 16–20 June 1987.
- TREFFERS, R. R., H. P. LARSON, U. FINK, AND T. N. GAUTIER 1978. Upper limits to trace constituents in Jupiter's atmosphere from an analysis of its 5- $\mu$ m spectrum. *Icarus* **34**, 331–343.